CeO 2 nanopowders as solid sorbents for efficient CO2 capture/release processes

Cedric Slostowski, Samuel Marre, Philippe Dagault, Odile Babot, Thierry Toupance, Cyril Aymonier

CeO_2 nano-powders as solid sorbents for efficient CO_2 capture/release processes

Cedric Slostowski[a], Samuel Marre[a], Philippe Dagault[a], Odile Babot[b], Thierry Toupance[b], Cyril Aymonier*[,a]

[a] CNRS, Univ. Bordeaux, ICMCB, UPR 9048, F-33600 Pessac (France)
[b] Institut des Sciences Moléculaires, Université de Bordeaux, UMR 5255 CNRS, C2M Team, 351 cours de la Libération, 33405 Talence (France)

KEYWORDS
Cerium oxide; CO_2 capture; Adsorption; Solid sorbent; High specific surface area.

ABSTRACT
Solid sorbents based on metal oxides have been investigated as an alternative to liquid sorbents for CO_2 capture. Amongst them, acid-base properties of cerium oxide make it an excellent candidate for such applications at rather low temperature. In order to assess the suitability of this material, we quantified CO_2 adsorption/desorption capacities at 25 °C and 0.1 MPa by TGA technique. The adsorption results show the importance of a preliminary thermal treatment of the sorbents under inert gas, in order to maximize CO_2 capture capacities *via* the thermal cleaning of CeO_2 surface (atmospheric and synthetic pollutants) liberating the access to CO_2 adsorption sites. CO_2 capture capacities depend on the specific surface area of the cerium oxide powders, reaching a maximum of 50 mg of CO_2 adsorbed per gram of CeO_2 displaying a specific surface area of 200 $m^2.g^{-1}$. The study also demonstrates the partial reversibility of this adsorption at 25 °C and its quantification, which can represent an important piece of information depending on the application (*e.g.*, catalysis or CO_2 capture). Finally, the CO_2 adsorption/desorption cycling of our best material was investigated exhibiting promising results for the use of CeO_2 powders as CO_2 solid sorbent with moderate temperature-swing conditions (between 25 °C and 150 °C).

INTRODUCTION

The reduction of greenhouse gases releases (*e.g.*, carbon dioxide – CO_2) has become an important challenge over the past 20 years, in order to reduce or prevent global warming and air pollution [1]. Several studies were conducted for selectively capturing CO_2 at emission points (industries), then releasing it afterwards for its storage (CCS: Carbon Capture and Storage) or reutilizing it as a raw material [2-4]. Two main approaches can be distinguished concerning the reversible capture of CO_2: (i) the use of liquid adsorbents solutions and (ii) the use of solid adsorbents.

The first approach is used in most of today's industrial processes but presents several limitations (*e.g.,* degradation of the liquid sorbent over temperature cycles causing regeneration costs) [5] that led industrials and scientists to look for alternative solutions *via* the use of solid sorbents, displaying various absorption capabilities (see Table 1 in the supporting information). From this perspective, new studies were conducted on the modification of the surface of materials by oxides (Cs, Ge, La, etc.) [6-8], or the utilization of these oxides alone [9-12], which displayed interesting properties for an efficient CO_2 reversible capture [13-14]. Carbon dioxide indeed possesses the capacity to strongly interact with the surface of these oxides. Among them, cerium oxide (CeO_2) displays interesting acid-base properties, which have been extensively studied by Lavalley *et al.* [15-22].

Based on FTIR analyses during temperature cycles on CeO_2 powders submitted to different gases, they showed that atmospheric pollutants (*e.g.*, water or carbon dioxide) can easily adsorb over cerium oxide surfaces at room temperature (RT), due to the high surface reactivity, making this material an excellent candidate for CO_2 capture (see Figure 1, 2 and Table 3 in the supplementary information). They demonstrated that the CO_2 captured over CeO_2 surface can adopt several configurations, each one of them displaying a different behavior over

temperature increase (CO_2 release). [17] While some configurations will be desorbed at room temperature, some of them may require temperatures up to 500 °C to be released. Thus, knowing that atmospheric carbon dioxide can graft onto CeO_2 surface at RT, along with atmospheric water, it appears essential to thermally treat CeO_2 powders at 500 °C under N_2, in order to fully activate CeO_2 NCs surfaces prior to CO_2 capture/release characterization. Several studies have been conducted in the past few years confirming or completing Lavalley *et al.* results [23-30].

While the interaction of cerium oxide with CO_2 has been described and used in many catalytic reactions [31-35], the quantification of the adsorption capacity has not been extensively studied yet. Recently, Yoshikawa et al. described the synthesis and analysis of CO_2 adsorbents based on cerium oxide, proposing for the first time a coherent quantification of the amount of CO_2 adsorbed [36]. In their study, they compared the CO_2 adsorption capacity of three different CeO_2 powders with other CO_2 adsorbents based on single-metal oxide, *i.e.* SiO_2, Al_2O_3 and ZrO_2. From their experimental results, several conclusions can be drawn concerning the important parameters to consider for CO_2 adsorption capacity on metal oxide materials.

First of all, the presence of chemical adsorption sites for CO_2 is obviously the most important parameter. Nevertheless, although SiO_2 exhibited the highest specific surface area (more than 800 $m^2.g^{-1}$), no CO_2 was adsorbed on this surface. The authors also showed that CeO_2-based materials exhibit the largest amount of CO_2 adsorbed in comparison with the other selected oxides.

It appeared that the adsorption capacity of CO_2 by CeO_2 is dependent on several parameters. The synthesis conditions, and especially the precursor used for the synthesis of the oxide, can generate pollutants on the surface of the oxide preventing the chemical adsorption of CO_2. Indeed, their materials synthesized from a chlorinated precursor displayed chloride pollutants over the surface, which they believe to reduce the adsorption capacity of the material (*via* the occupation of adsorption sites). Morphology, particle sizes, porosity and specific surface area of the materials are also important parameters determining the capture efficiency. Such parameters conditioned not only the number of adsorption sites available for the CO_2 chemical adsorption but also the accessibility of these sites to CO_2 molecules.

The more efficient material they tested towards the CO_2 adsorption was a commercial high-surface-area CeO_2 powder (specific surface are – S_{spe} = 166 $m^2.g^{-1}$) which is able to adsorb around 5.7 mg of CO_2 per gram of CeO_2 (130 $mmol.g^{-1}$) at 50 °C. Their study also provided results similar to those of Lavalley *et al.* concerning the kind of carbonate species interacting with the surface of CeO_2 during the adsorption and desorption of CO_2.

Another study by Li *et al.* [36bis] reports the capture of CO_2 on CeO_2 nanopowders prepared by a surfactant-templated method over the CO_2 absorption capacity at room temperature. The results obtained with pure CeO_2 are slightly higher, namely: 700 mmol.g-^{1} (*i.e.* ~30 mg/g) for S_{spe} = 181 $m^2.g^{-1}$.

In our previous work, we described the fast and simple synthesis in near- and supercritical alcohols of CeO_2 nanocrystals aggregated in bigger round shapes [37]. We showed that our powders can display high specific surface area – up to 200 $m^2.g^{-1}$ – and keep their particular morphology, after a thermal treatment at 500 °C, required to clean the surface of the CeO_2 powders [38]. Thus, our CeO_2 nanocrystals appear to be excellent candidates as CO_2 solid adsorbents. In this work, we propose a method to quantify the adsorption and the desorption of CO_2 over cerium oxide powders at 25 °C and 0.1 MPa, and to draw a relation between the specific surface area of the powders and their CO_2 adsorption capacity, while demonstrating that an appropriate thermal treatment of the CeO_2 powders is of key importance in order to maximize the activity of CeO_2 towards CO_2 capture.

EXPERIMENTAL SECTION

Materials. The CeO_2 powders used in this work were previously synthesized in our custom-built continuous process and characterized, as described in our previous work [37]. As a reminder, they were synthesized from ammonium cerium nitrate in near- or supercritical alcohols: methanol (scMeOH), ethanol (scEtOH), propanol (scPrOH), butanol (scButOH), pentanol (ncPentOH), hexanol (ncHexOH) and isopropanol (sciPrOH). The experimental

conditions were set at 300 °C and 24.5 MPa, with a residence time (t_s) of 55 s. The recovered dry powders were used as produced, without any post-treatment.
Three additional samples of CeO_2 powders synthesized in near- and supercritical water were also studied as a matter of comparison with powders synthesized in alcohols [37]. The experimental conditions were set at 300 °C, 24.5 MPa and 45 s for the first sample and 400 °C, 24.5 MPa, 10 s and 45 s for the two other samples. The recovered dry powders were also used as produced.
All dry powders were grinded and sieved before further utilization.
The synthesis conditions, the crystallite sizes and the specific surface areas of the as-synthesized CeO_2 nanocrystals (NCs) are reminded in Table 2 of Supplementary information, along with their crystallite sizes and specific surface areas after 5 h of thermal treatment under N_2.
The nitrogen flow was provided by the internal gas network in our laboratory, while the CO_2 (purity ≥ 99.5%) was purchased from Air Liquide and filtrated through a SiO_2 sieve tank prior to utilization.

Apparatus and procedure.
Thermal treatment under N_2 flow and CO_2 capture quantification were both performed using a TGA apparatus equipped with a custom-built gas inlet. Approximately 100 mg of CeO_2 powders were placed in a Pt crucible, itself placed in a microbalance SETARAM *mtb 10-8*. A schematic representation of the apparatus is given in Figure 1. The 3-way valve allows switching from N_2 to CO_2 during TGA analysis.

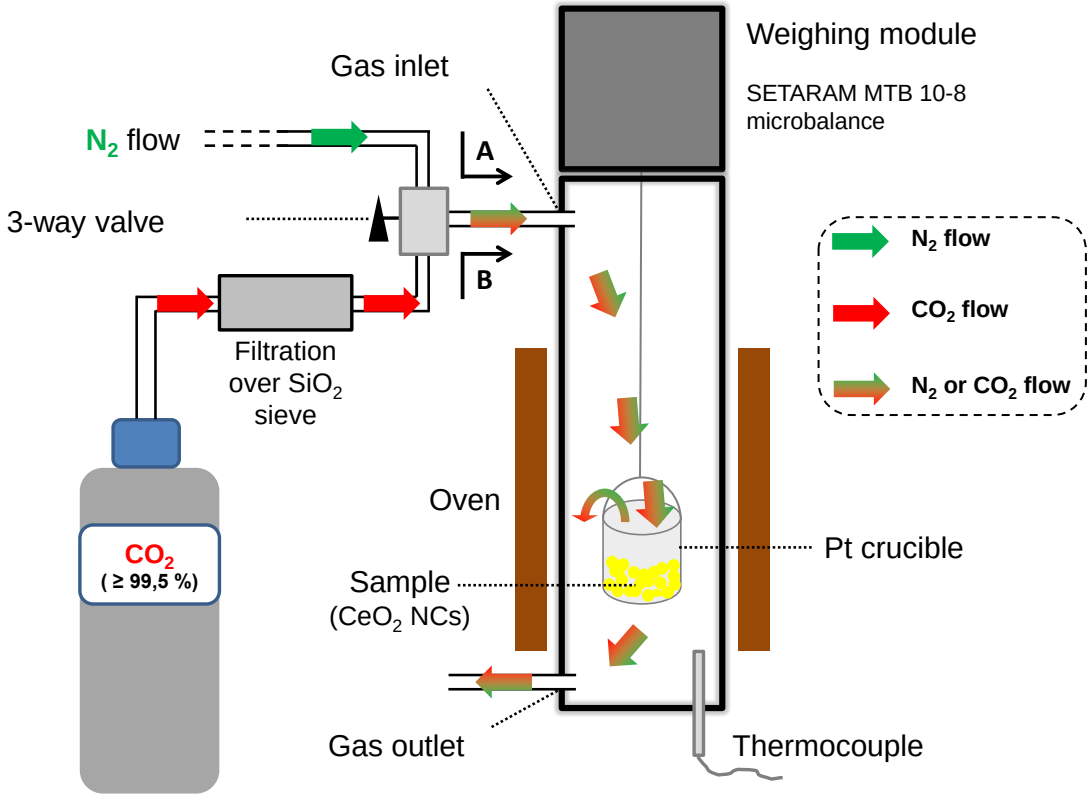

Figure 1. Schematic representation of the TGA apparatus used for CeO_2 powders thermal treatment under N_2 flow (*Gas path* ***A***) and the quantification of CO_2 capture over CeO_2 nanopowders (*Gas path* ***B***)

Prior to the CO_2 capture quantification analysis, CeO_2 powders are submitted to a thermal treatment under a N_2 flow (Figure 1 – *Gas path* ***A***). First, the temperature is maintained for 1 h at room temperature (RT), in order to stabilize the microbalance atmosphere, before being

raised at 5 °C.min^{-1} up to 500 °C. Then, the temperature is kept constant (500 °C) for 5 h, before being finally decreased to RT at 5 °C.min^{-1}.
Once the temperature is back to RT, a CO_2 flow is injected into the microbalance for 3 h at RT (*Gas path* ***B***), in order to quantify the CO_2 capture over the CeO_2 powders. Finally, the gas flow is switched back to N_2 (*Gas path* ***A***), in order to quantify the CO_2 desorption from the CeO_2 surface.

Characterization techniques. Crystallite sizes (d_{cr}) of the CeO_2 nanocrystals were calculated using XRD patterns. The XRD patterns were recorded on a PANalytical X'Pert MPD powder diffractometer (θ−θ Bragg−Brentano geometry using Cu $K_{\alpha1,\alpha2}$ (λ_1 = 1.54060 Å, λ_2 = 1.54441 Å) radiation, equipped with a secondary monochromator and a X'Celerator detector, in the range of 8−120°, in continuous scan mode at 3.5 × 10^{-3} °·s^{-1}. The powder was ground and sieved at 50 µm before being subjected to XRD.
The texture of the CeO_2 nanocrystals was analyzed by nitrogen adsorption isotherm (77 K) measurements. Data collection was performed by the static volumetric method, using an ASAP2010 apparatus (Micromeritics). Prior to each measurement, the samples were degassed at 150 °C in *vacuo* for a time interval high enough to reach a constant pressure (<10 µmHg). The BET equation was applied between 0.05 and 0.3 relative pressures to provide specific surface areas (S_{sp}).

RESULTS

Characterization and quantification of the CO_2 adsorption/desorption over thermally treated CeO_2 powders synthesized in nc- or sc-alcohols. CO_2 captured over CeO_2 can adopt several configurations, as it has been demonstrated by Lavalley *et al.* [17] (see Figure 1 of Supplementary information). Depending on the configuration adopted by the CO_2 over the CeO_2 surface, its release may require temperatures up to 500 °C. Knowing that atmospheric carbon dioxide can graft onto CeO_2 surface at RT, along with atmospheric water, it appears essential to thermally treat CeO_2 powders at 500 °C under N_2, in order to fully activate the CeO_2 NCs surfaces prior to CO_2 capture/release characterization.
Thus, CeO_2 powders were submitted to a 5 h thermal treatment at 500 °C under N_2, as previously described, prior to the CO_2 capture/release characterization. Once the temperature is back to RT, the CeO_2 samples were submitted to a CO_2 flow at RT (Figure 1 – *Gas path* ***B***) for 3 h, in order to quantify carbon dioxide adsorption over the CeO_2 surfaces. Finally, gas is switched to N_2 for 3 h at RT, in order to quantify CO_2 desorption from CeO_2 surfaces. Weight losses of samples over such treatment cycle are followed by TGA measurements.
All the analyzed CeO_2 powders adopted the same behavior when submitted to such treatment. A general representation of the behavior of these powders is given in Figure 2, along the gas/temperature program used.
During the preliminary thermal treatment under N_2 flow, a drastic weight loss is observed. This phenomenon can be attributed to water and carbon dioxide desorption, which can graft easily at RT, but also to grafted alcohol desorption. Indeed, we previously showed that the alcohol used as solvent during the synthesis in near- or supercritical conditions acts as a surface modifier for the CeO_2 surfaces [37,39], and tends to desorb in this temperature range [38].
Then, when CO_2 is flown over the CeO_2 NCs at RT, a gain in weight is observed, which is attributed to CO_2 adsorption over the CeO_2 surfaces. Finally, a weight loss is witnessed when atmosphere is switched back to N_2 flow, corresponding to a partial desorption of CO_2 from the CeO_2 surfaces.

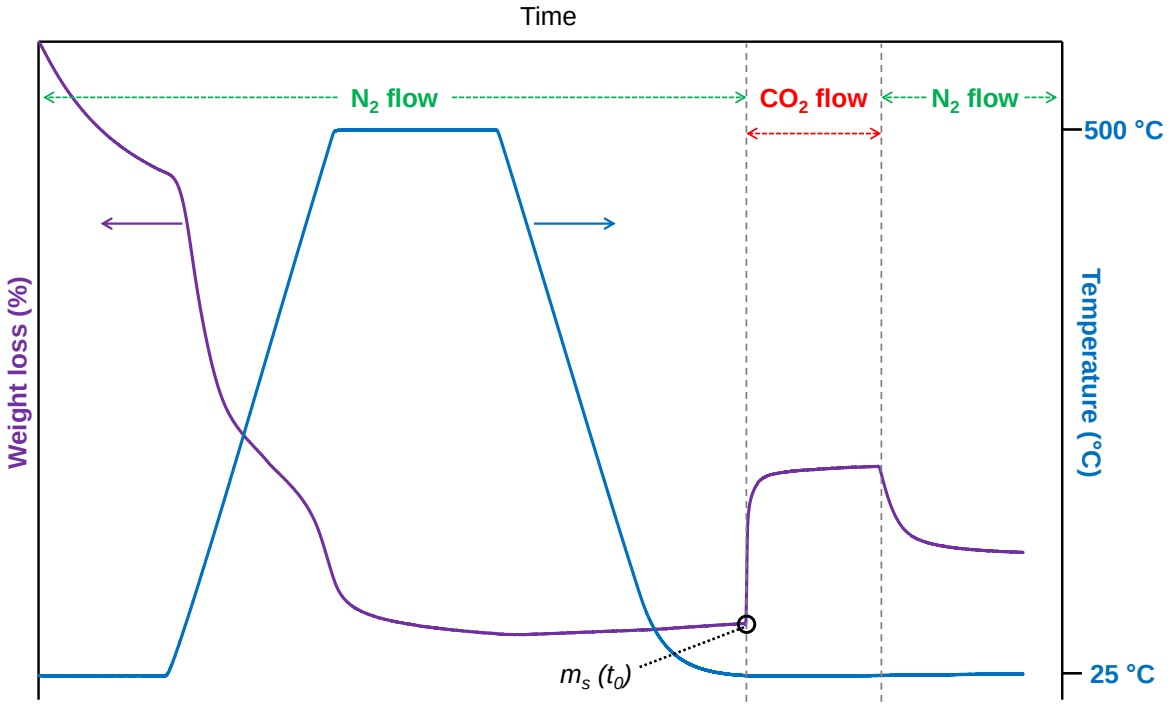

Figure 2. Representation of the general behavior for the weight loss of CeO_2 powders monitored by TGA. The sample is treated under **N_2** at RT for 1 h then at 500 °C for 5 h (5 °C.min^{-1}). Back to RT, the sample is submitted to a **CO_2** flow for 3 h then to a **N_2** flow for 3 h. $m_s(t_0)$: Initial weight of the sample when atmosphere is switched to **CO_2**.

The adsorption capacity of CO_2 for each sample as the function of time ($Ads_{CO2}(t)$, in mg of CO_2/g of CeO_2, or mg/g) can be calculated from the TGA curves. The mass of the sample at the beginning of CO_2 flow switch ($m_s(t_0)$, in mg) is used as a reference (**Figure 2**). The mass of CO_2 adsorbed by the CeO_2 as a function of time ($m_{CO2\text{-}ads}(t)$, in mg) can be therefore obtained by subtracting the initial mass $m_s(t_0)$ to the mass at the time *t* ($m_s(t)$, in mg), as described by the Equation (1).
Thus, the adsorption capacity of CO_2 by the sample as a function of time ($Ads_{CO2}(t)$) is easily calculated as the ratio of the mass of CO_2 adsorbed by the sample over the mass at t_0 (Equation (2)).

$$m_{CO_2\text{-}ads}(t) = m_s(t) - m_s(t_0) \quad (1)$$

$$Ads_{CO_2}(t) = \frac{100 \cdot m_{CO_2\text{-}ads}(t)}{m_s(t_0)} \quad (2)$$

Based on these considerations, a general representation of the variation of the CO_2 quantity adsorbed on the CeO_2 surface as a function of time ($Ads_{CO2}(t)$) is given in Figure 3. Several observations and conclusions can be withdrawn from such curve.
First, as observed by Lavalley *et al.* [17], about 15 min are needed to reach the maximum CO_2 adsorption quantity (Ads_{max}, in mg CO_2/g CeO_2). Such phenomenon is led by both the diffusion kinetics of CO_2 in the material and the thermodynamics of CO_2-CeO_2 interactions.
When the atmosphere is switched from a CO_2 to a N_2 flow, a decrease of the adsorbed CO_2 quantity is observed. Yet, this phenomenon is not only slower than the adsorption but also not complete, *i.e.* a considerable amount of CO_2 remains adsorbed over CeO_2 surfaces after several hours of N_2 flow at 25 °C. Regarding the works of Lavalley *et al.*, such phenomenon can easily be explained by the broad range of CO_2-CeO_2 interaction species forming during the adsorption at 25 °C under a CO_2 flow (Figure 1 of Supplementary information). Some of them will desorb spontaneously at 25 °C when the CO_2 flow is stopped (*i.e.*,

hydrogenocarbonates and bridged carbonates mainly) while other will require temperatures up to 500 °C to be desorbed (*i.e.*, bidentate, monodentate and polydentate carbonates mainly).

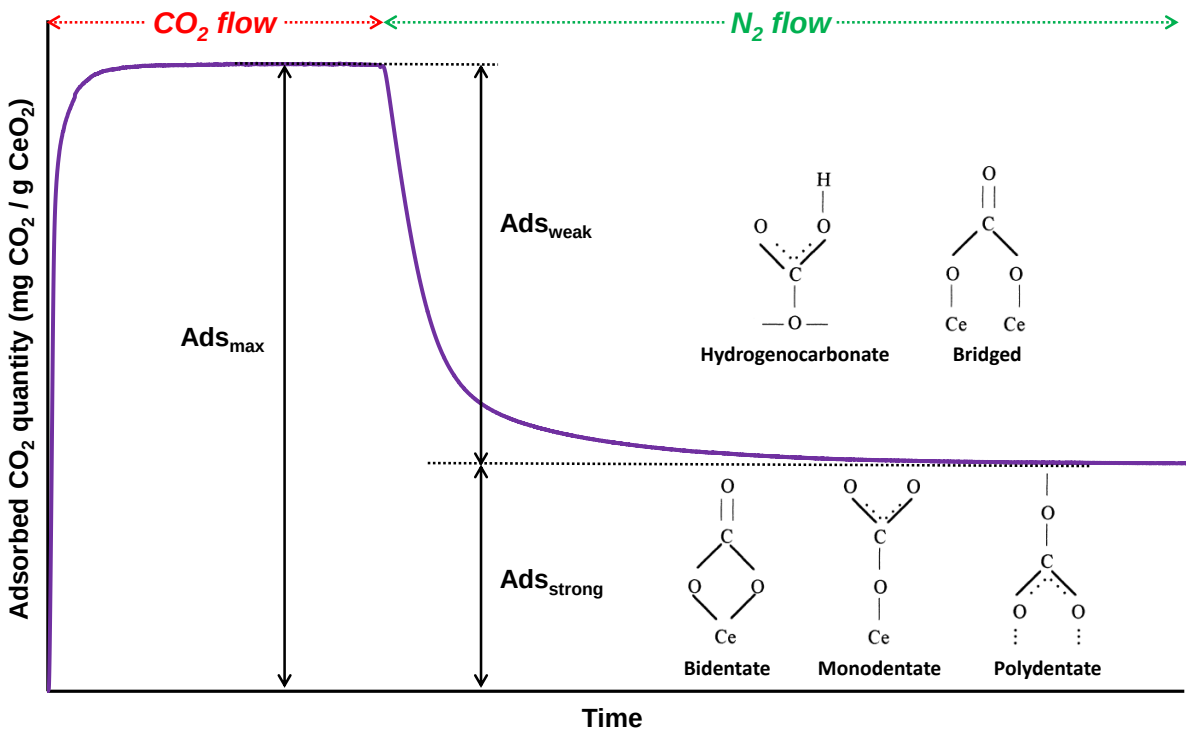

Figure 3. General overview of the quantity of adsorbed CO_2 over CeO_2 samples as a function of time. Representations of the most probable configurations for CO_2-CeO_2 interactions are also pictured. Hydrogenocarbonates and bridged carboxylates are desorbed at RT under N_2 flow (weak CO_2 adsorption, Ads_{weak}). Bidentate, monodentate and polydentate carboxylates remains at the surface of CeO_2 after N_2 flow at RT (strong CO_2 adsorption, Ads_{strong}).

Thus, the maximum quantity of CO_2 adsorbed can be considered as the sum of two kinds of CO_2 interactions with CeO_2 surface. First, the hydrogenocarbonates and bridged carbonates form weak interactions at 25 °C, and desorb by simply stopping the CO_2 flow over the CeO_2 samples. Those species can be quantified as the quantity of CO_2 desorbed from CeO_2 surfaces during the purge at 25 °C (Ads_{weak}, in mg CO_2/g CeO_2, or mg/g). Then, bidentate, monodentate and polydentate carbonates create a strong interaction with CeO_2 surfaces and cannot be desorbed from these surfaces at 25 °C. They can be quantified as the quantity of CO_2 still adsorbed over CeO_2 surfaces during the purge at 25 °C (Ads_{strong}, in mg CO_2/g CeO_2, or mg/g). Such differentiation can be very useful for applications such as CO_2 storage, which may require a stable adsorption even when CO_2 flow is stopped (*i.e.*, Ads_{strong}) or which may require CO_2 desorption at low temperatures (Ads_{weak}), depending on the utilization.
The experimental values of Ads_{max} and Ads_{strong} are plotted as a function of the CeO_2 NCs specific surface area in **Figure 4** (The exact values can be found in Table 3 of the Supplementary information, along with those of the Ads_{weak}).
The cerium oxide powders synthesized in near- and supercritical alcohols allow reaching a maximum quantity of adsorbed CO_2 up to 48 mg/g of CeO_2, for samples developing high specific surface areas.

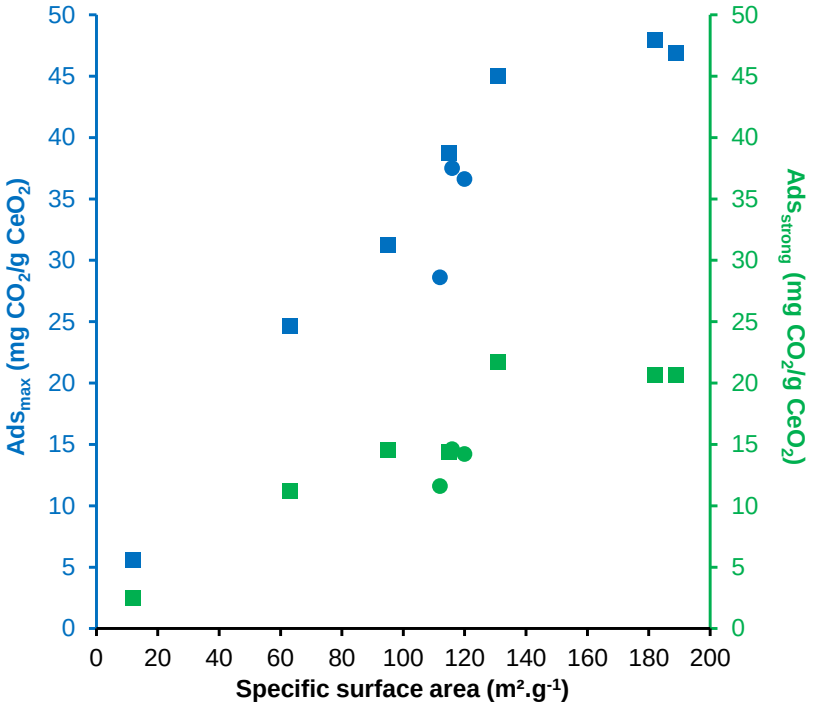

Figure 4. Experimental values of the Ads_{max} and the Ads_{strong} as a function of the surface specific areas of the CeO_2 powders thermally treated at 500 °C under N_2 flow. Squares are CeO_2 powders synthesized in nc- or sc-alcohols and circles the ones synthesized in nc- or sc-water.

CeO_2 powders synthesized in near- and supercritical water have also been submitted to the same N_2 thermal treatment at 500 °C and CO_2 adsorption/desorption cycle at RT. Similar behaviors are observed and the measured Ads_{max} validate that it exists a relationship between the quantity of CO_2 adsorbed over CeO_2 surfaces and the specific surface area, disregarding their syntheses conditions. The Ads_{max} and Ads_{strong} of these samples as a function of their specific surface areas are presented in Figure 4, along with the results with alcohols (The exact values can also be found in Table 4 of the Supplementary information, along with those of the Ads_{weak}).

DISCUSSION

Concerning the CO_2 adsorption capacity of the thermally treated CeO_2 NCs, the TGA analyses under CO_2 flow at 25 °C showed that the maximum quantity of CO_2 adsorbed on the surface of CeO_2 NCs increases linearly with the specific area of CeO_2 powders in the range 0-150 $m^2.g^{-1}$. This work is the first demonstration of such a relationship between CO_2 adsorption capacity over CeO_2 and specific surface area.

However, we noticed that this adsorption reaches its limits at 48 mg of CO_2 captured by gram of CeO_2 powders (synthesized in ncHexOH). But this limit appears at high specific areas, when ButOH, PentOH and HexOH are used for the synthesis. Now, we previously showed that not all organic species are desorbed from such CeO_2 samples at 500 °C, which limits their specific surface areas but also makes a hard path for CO_2 diffusion through the round shaped structures.

Playing with thermal treatment to increase the adsorption rates. Our previous work showed that a treatment under N_2 flow at a temperature higher than 500 °C can enhance the desorption of organic species and thus leads to CeO_2 NCs with higher specific surface areas [38]. Nonetheless, a temperature too important can also lead to sintering which will have the opposite effect, *i.e.* a decrease of the specific surface areas of the materials.

This treatment temperature also plays an important role to improve the CO_2 adsorption capacities of the CeO_2 powders, alongside with the specific surface areas of the materials. As previously shown, the CeO_2 NCs synthesized in ncHexOH reach a S_{sp} of 182 $m^2.g^{-1}$ and display

an Ads_{max} of 47.9 mg/g after a thermal treatment at 500 °C. When submitted to a thermal treatment at 540 °C, the S_{sp} of these materials increases from 182 to 199 $m^2.g^{-1}$ owing to a better desorption of surface pollutants and the Ads_{max} also increases alongside from 47.9 mg/g versus 49.6 mg/g. On the contrary, the CeO_2 NCs exposed to a thermal treatment at 600 °C undergo sintering and thus, the S_{sp} of these materials decreases (from 199 $m^2.g^{-1}$ to 185 $m^2.g^{-1}$) and the Ads_{max} declines accordingly from 47.9 mg/g to 36.7 mg/g. The Ads_{weak} and Ads_{strong} of these materials are given in the Table 5 of Supplementary information.

These results show the importance of choosing an appropriate temperature for the thermal activation of the CeO_2 (mandatory to remove surface pollutants and thus activate the material towards CO_2 capture) prior to their use for CO_2 capture.

Cyclability of the CeO_2 powders. We have further investigated the suitability of our materials as potential CO_2 solid sorbents by checking their cyclability. Indeed, we showed that our materials can display high specific surface area and interesting CO_2 adsorption capacity at low temperature (25 °C and 0.1 MPa), but to be suitable as CO_2 solid sorbents, they need to be regenerable for continuous use with an acceptable thermal treatment cycle.

In this regard, a longer experiment was led on crude CeO_2 powders synthesized in ncHexOH with 3 CO_2 adsorption tests and different regeneration steps under N_2. The weight loss of the sample and thus, its CO_2 adsorption/desorption during this experiment were followed by TGA and the results are presented in Figure 5, along with the experimental conditions (temperature, time and gas flow). Numerical values of these results are also given in Table 1.

The first step was a classical thermal treatment at 500 °C under N_2 flow in order to eliminate pollutants from the surface of CeO_2 powders, resulting in a weight loss from the sample (-12.7 %). Of course, this temperature is not sufficient to achieve a complete desorption of the pollutants, as previously demonstrated, but allows avoiding the sintering of the powders. Once the sample is back to RT, the gas flow was switched to CO_2 (Step 2), which resulted in a gain of weight of the sample (+ 3.8 %), corresponding to an adsorption of 44.0 mg of CO_2 per gram of CeO_2, which is comparable to the value previously obtained with similar treatment and samples (Table 2 of Supplementary information).

In a third step, gas flow was switched back to N_2 to characterize the CO_2 desorption from the sample at 25 °C. It resulted in a weight loss of the sample (- 2.0 %) corresponding to a CO_2 desorption of 24.0 mg/g, which is in good agreement with previous experiments.

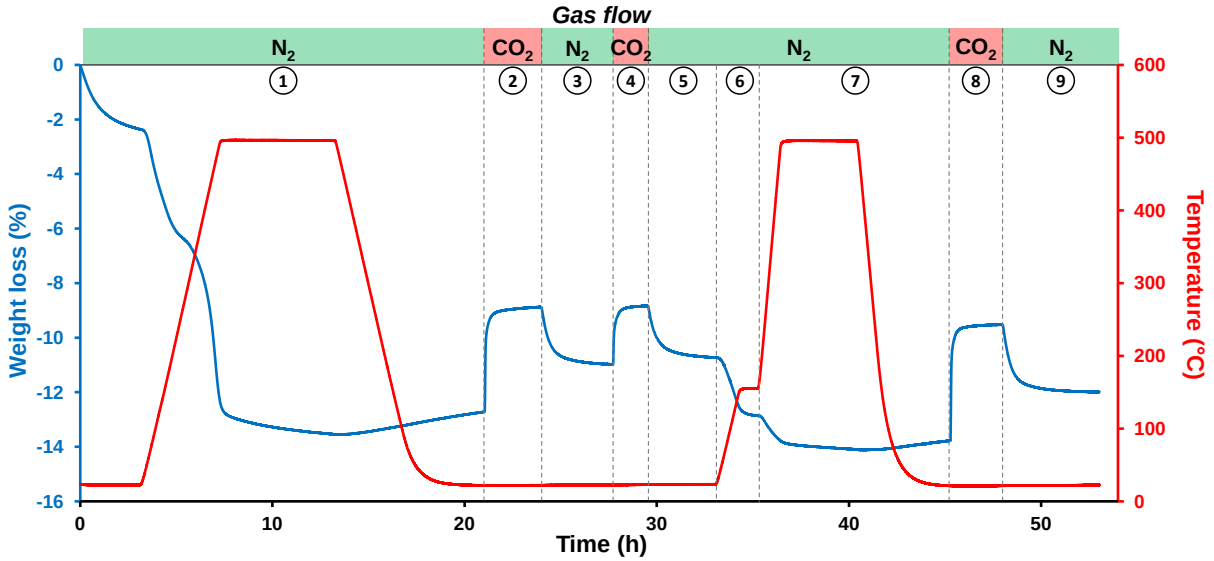

Figure 5. Experimental conditions and weight loss of CeO_2 powders synthesized in ncHexOH and submitted to cycling tests of CO_2 adsorption/desorption.

Another CO_2 adsorption/desorption cycle at RT was then performed in order to compare the values of Ads_{weak} for pristine and reused CeO_2 powder (Step 4). A gain of weight of + 2.0 % was witnessed corresponding to an adsorption of 24.4 mg of CO_2 per gram of CeO_2. This

means that all the CO_2 that was desorbed during the previous step under N_2 at 25 °C can be adsorbed again at the CeO_2 surface, *i.e.* there is no loss of CO_2 adsorption capacity after a desorption step at 25 °C. This CO_2 is once again desorbed under N_2 flow at 25 °C during a fifth step (weight loss of - 1.9 %, *i.e.* a CO_2 desorption of 22.6 mg/g during this step). This may mean that each CeO_2 adsorption sites will favor a specific type of interaction for the capture of CO_2 (*e.g.*, hydrogenocarbonate or bidentate carbonate) which remains the same over cycling.

Table 1. Cycling experiments performed on the CeO_2 powders synthesized in ncHexOH.

Step	Gas	T (°C)	Duration (h)	Total weight loss (%)[a]	ΔAds(CO_2) (mg/g)[b]
1	N_2	25	3	- 12.7	-
		25 to 500	4		
		500	6		
		500 to 25	7		
		25	1		
2	CO_2	25	3	- 8.9	+ 44.0
3	N_2	25	4	- 10.9	- 24.0
4	CO_2	25	2	- 8.9	+ 24.4
5	N_2	25	4	- 10.8	- 22.6
6	N_2	25 to 150	1	- 12.9	- 24.2
		150	1		
7	N_2	150 to 500	2	- 13.7	-
		500	4		-
		500 to 25	4		-
		25	1		-
8	CO_2	25	3	- 9.5	+ 49.3
9	N_2	25	5	-12.0	- 20.7

[a] *Total weight loss of the material recorded from the beginning of the experiment by TGA.*
[b] *Calculated values of the adsorption (positive values) and desorption (negative values) of CO_2 by CeO_2 powders, deduced from the total weight loss values. The ΔAds(CO_2) values are cumulative, which means that after the Step 3, for example, 24.0 mg of CO_2 per gram of CeO_2 are desorbed (Ads_{weak} = 24 $mg.g^{-1}$) while (+44.0 + (-24.0) =) 20.0 mg of CO_2 per gram of CeO_2 remain on CeO_2 powders (Ads_{strong} = 20 $mg.g^{-1}$).*

A desorption temperature of 25 °C is obviously not sufficient enough to desorb all the CO_2 captured by the CeO_2 powders. Indeed, the work of Lavalley *et al.* showed that the CO_2 species adsorbed at the surface of CeO_2 can require temperatures up to 500 °C to be desorbed [17]. A temperature difference of 475 °C (between 25 °C for the CO_2 adsorption and 500 °C for the CO_2 desorption) would hardly make CeO_2 suitable as a solid sorbent from an energy point of view compared to classical use of liquid monoethanolamine, which can adsorb CO_2 at 25 °C and can be regenerated at 150 °C. Fortunately, not all CO_2 species required temperature of 500 °C to desorb and some of the species, which do not desorb at RT, could be desorbed around 150 °C, according to the work Lavalley *et al.*.
In order to check what could be the desorption efficiency with a thermal treatment at 150 °C (comparable to conventional liquid sorbent desorption process), a sixth step was performed under N_2 with a 1 h threshold at 150 °C. A weight loss of – 2.1 % is observed during this step, corresponding to a CO_2 desorption of 24.2 mg/g. Unexpectedly, this temperature increase from 25 °C to 150 °C under N_2 flow allows retrieving the weight of CeO_2 in presence after the initial

N_2 thermal treatment (500 °C) and before the two CO_2/N_2 cycles at 25 °C. This means that the amount of CO_2 species present at the surface in the CeO_2 powders, which requires a thermal treatment over 150 °C, is negligible. Thusly, CeO_2 powders would make great candidate at low temperature as CO_2 solid sorbent for replacing liquid adsorbent systems.
Then, a seventh step was performed under N_2 flow with a 4 h threshold at 500 °C, witnessing a weight loss of - 0.8 % after the temperature is back to RT. This weight loss is attributed to desorption of remaining organic species from the synthesis (alcohol grafts). This hypothesis is confirmed by the gain in weight (+ 4.2 %) observed during a final step (Step 8) under CO_2 at 25 °C (Step 8), which corresponds to a CO_2 adsorption of 49.3 mg/g. This adsorption capacity is higher than the one recorded after the first CO_2 adsorption (Step 2, 44.0 mg/g), which is **coherent** with the previous hypothesis. Indeed, not all the organic species from the synthesis are desorbed during the first step at 500 °C under N_2, which limits the CO_2 adsorption capacity of the material. During this second threshold at 500 °C (Step 7), more surface pollutants are removed from the surface creating more available adsorption sites for CO_2 and thus increasing the maximum CO_2 adsorption capacity of the CeO_2 powders.
In brief, cerium oxide powders with high specific surface areas appear as great candidates for temperature-swing reversible capture of CO_2 at low temperature – between 25 and 150 °C – compared to most of the other metal oxides studied so far, which required higher temperatures for cyclability (*e.g.*, $CaO/CaCO_3$ between 700 and 800 °C [2,40]). This dramatically enhances the energy efficiency of the process.

CONCLUSION

The suitability of CeO_2 materials as CO_2 solid sorbent has been examined on powders displaying a large array of different specific surface areas (from 12 up to 199 $m^2.g^{-1}$). This study showed that the adsorption efficiency of the CeO_2 materials is primarily dependent on its specific surface area, with an almost linear relationship.
The adsorption of CO_2 requiring the access of CO_2 to the surface atoms of CeO_2, we also showed that a thermal activation of the materials before their use as a solid sorbent is mandatory. This thermal treatment requires knowing well the material in order to wisely choose the operating temperature and thusly, maximize the CO_2 capture capacity of the materials. Indeed, the preliminary treatment temperature must respect two major conditions: (i) being high enough to remove most of the surface pollutants from the material (*e.g.*, atmospheric water and CO_2 and synthesis residues), which are blocking potential CO_2 adsorption sites and (ii) being low enough to avoid the sintering of the material, which will drastically decrease the CO_2 adsorption capacity of the material along with its specific surface area [38].
This way, our CeO_2 powders, displaying a specific surface area of 199 $m^2.g^{-1}$ after a thermal treatment at 540 °C under N_2 flow, exhibited at 25 °C and 0.1 MPa a maximal CO_2 adsorption capacity around 50 mg of CO_2 per gram of CeO_2 (*i.e.*, around 1130 mmol of CO_2/kg of CeO_2). It was also demonstrated that the adsorption of CO_2 by CeO_2 is partially reversible at 25 °C and gave a quantification of the CeO_2-CO_2 species that can be desorbed just by stopping the CO_2 flow and those which remains at the surface. Such distinction may be of key importance depending on the sought application for this material, *e.g.* catalysis requiring weak adsorption or capture requiring strong adsorption.
Eventually, the possible CO_2 adsorption/desorption cycling over CeO_2 powders has been examined. The preliminary analyses show that it is possible to adsorb CO_2 at 25 °C and to regenerate almost completely the material at 150 °C under inert gas atmosphere, without losing the CO_2 capture capacity. That way, we believe that high specific surface area CeO_2 materials can be future great candidates as reversible low temperature CO_2 solid sorbents (25 – 150 °C), making them competitive alternative to conventional liquid sorbents systems.

AUTHOR INFORMATION

Corresponding Author
*Mailing address: ICMCB-CNRS, 87 Avenue du Dr Albert Schweitzer, 33608 Pessac Cedex, France. E-mail: cyril.aymonier@icmcb.cnrs.fr

Notes
The authors declare no competing financial interest.

ACKNOWLEDGMENTS
The authors acknowledge the “Conseil Régional d’Aquitaine” for funding the PhD grant of C. Slostowski.

REFERENCES
[1] IPCC, 2014: Climate Change 2014: Synthesis Report. Contribution of Working Groups I, II and III to the Fifth Assessment Report of the Intergovernmental Panel on Climate Change. IPCC, Geneva, Switzerland, 151 pp.
[2] S. Choi, J. H. Drese, C. W. Jones, ChemSusChem 2 (2009) 796-854
[3] H. Yang, Z. Xu, M. Fan, R. Gupta, R. B. Slimane, A. E. Bland, I. Wright, J. Environ. Sci. 20 (2008), 14-27
[4] S.-Y. Lee, S.-Y. Park, J. Ind. Eng. Chem. 23 (2015) 1-11
[5] C.-H. Yu, C.-H. Huang, C.-S. Tan, Aerosol Air Qual. Res. 12 (2012) 745-769
[6] J. Chang Kim, H.-X. Li, C.-Y. Chen, M. Davis. Microporous Mater. 2 (1994) 413–423
[7] P. Hathaway, M. Davis. J. Catal. 116 (1989) 263–278
[8] R. Roque-Malherbe, R. Polanco-Estrella, F. Marquez-Linares. J. Phys. Chem. C 114 (2010) 17773–17787
[9] F. Garcia-Labiano, A. Abad, L. de Diego, P. Gayan, J. Adanez. Chem. Eng. Sci. 57 (2002) 2381–2393
[10] Y. Lin, Q. Yang, J. Ida. J. Taiwan Inst. Chem. Eng. 40 (2009) 276–280
[11] W. Liu, N. Low, B. Feng, G. Wang, J. Diniz Da Costa. Environ. Sci. Technol. 44 (2010) 841–847
[12] C.-H. Huang, K.-P. Chang, C.-T. Yu, P.-C. Chiang, C.-F. Wang. Chem. Eng. J. 161 (2010) 129–135
[13] R. Bal, B. Tope, T. Das, S. Hegde, S. Sivasanker. J. Catal. 204 (2001) 358–363
[14] J.-C. Lavalley, Catal. Today 27 (1996) 377–401
[15] C. Binet, A. Badri, M. Boutonnet-Kizling, J.-C. Lavalley. J. Chem. Soc., Faraday Trans. 90 (1994) 1023–1028
[16] M. Daturi, C. Binet, J.-C. Lavalley, H. Vidal, J. Kaspar, M. Graziani, G. Blanchard. J. Chim. Phys. Phys.-Chim. Biol. 95 (1998) 2048–2060
[17] C. Binet, M. Daturi, J.-C. Lavalley. Catal. Today 50 (1999) 207–225
[18] M. Daturi, C. Binet, J.-C. Lavalley, A. Galtayries, R. Sporken. Phys. Chem. Chem. Phys. 1 (1999) 5717–5724
[19] M. Daturi, E. Finocchio, C. Binet, J.-C. Lavalley, F. Fally, V. Perrichon. J. Phys. Chem. B 103 (1999) 4884–4891
[20] M. Daturi, C. Binet, J.-C. Lavalley, G. Blanchard. Surf. Interface Anal. 30 (2000) 273–277
[21] M. Daturi, E. Finocchio, C. Binet, J.-C. Lavalley, F. Fally, V. Perrichon, H. Vidai, N. Hickey, J. Kaspar. J. Phys. Chem. B 104 (2000) 9186–9194
[22] C. Binet, M. Daturi. Catal. Today 70 (2001) 155–167
[23] J. Stubenrauch, E. Brosha, J. Vohs, Catal. Today 28 (1996) 431–441
[24] K. Hadjiivanov, G. Vayssilov, Adv. Catal. 47 (2002) 307–511
[25] G. Jacobs, L. Williams, U. Graham, G. Thomas, D. Sparks, B. Davis, Appl. Catal., A 252 (2003) 107–118
[26] M. Swanson, V. Pushkarev, V. Kovalchuk, J. D’itri, Catal. Lett. 116 (2007) 41–45
[27] W. Gordon, Y. Xu, D. Mullins, S. Overbury. Phys. Chem. Chem. Phys. 11 (2009) 11171–11183
[28] Y. Lykhach, T. Staudt, R. Streber, M. Lorenz, A. Bayer, H.-P. Steinruck, J. Libuda, Eur. Phys. J. B 75 (2010) 89–100
[29] G. Vayssilov, M. Mihaylov, P. Petkov, K. Hadjiivanov, K. Neyman, J. Phys. Chem. C 115 (2011) 23435–23454
[30] Y. Zhai, S. Zhang, H. Pang, Mater. Lett. 61 (2007) 1863–1866
[31] A. Trovarelli, Catal. Rev. 38 (1996) 439-520

[32] R. Juarez, P. Concepcion, A. Corma, H. Garcia, Chem. Commun. 46 (2010) 4181–4183
[33] K. Rao, B. Reddy, S.-E. Park, Appl. Catal., B 100 (2010) 472-480
[34] K. Reed, A. Cormack, A. Kulkarni, M. Mayton, D. Sayle, F. Klaessig, B. Stadler, Environ. Sci.: Nano 1 (2014) 390–405
[35] C. Walkey, S. Das, S. Seal, J. Erlichman, K. Heckman, L. Ghibelli, E. Traversa, J. F. McGinnis, W. T. Self, Environ. Sci.: Nano 2 (2015) 33–53
[36] K. Yoshikawa, H. Sato, M. Kaneeda, J. N. Kondo, J. CO_2 Util. 8 (2014) 34-38.
[36bis] M. Li, U. Tumuluri, Z. Wu, S. Dai, *ChemSusChem*, 2015, 8, 3651-3660
[37] C. Slostowski, S. Marre, O. Babot, T. Toupance, C. Aymonier, Langmuir 28 (2012) 16656–16663.
[38] C. Slostowski, S. Marre, O. Babot, T. Toupance, C. Aymonier, ChemPhysChem (2015), doi:10.1002/cphc.201500570 in press
[39] C. Slostowski, S. Marre, O. Babot, T. Toupance, C. Aymonier, Langmuir 30 (2014) 5965–5972
[40] E.T. Santos, C. Alfonsín, A.J.S. Chambel, A. Fernandes, A.P. Soares Dias, C.I.C. Pinheiro, M.F. Ribeiro, Fuel 94 (2012) 624–628